

1 Supporting Information

2 **PHOTOCHEMICAL PRODUCTION AND PHOTOLYSIS OF ACRYLATE IN**
3 **SEAWATER**

4
5
6 Lei Xue and David J. Kieber*

7
8
9
10
11
12
13
14
15 Department of Chemistry, State University of New York, College of Environmental Science and
16 Forestry, 1 Forestry Drive, Syracuse, New York 13210

17
18
19
20
21
22 *Corresponding Author: djkieber@esf.edu, Phone: 1-315-470-6951, Fax: 1-315-470-6856

23
24 Supporting Information is 10 pages including 6 figures and 1 table

26 **S1 Determination of Hourly Rates.** Average, clear-sky photochemical production rates were
27 determined by first dividing the nM of acrylate produced during a photochemical experiment by
28 the hours samples were exposed to solar radiation. Observed hourly rates were then scaled to
29 rates that would be expected under cloudless, clear-sky conditions on days that the
30 photochemical experiments were conducted. This was done by dividing hourly rates by the ratio
31 of the photon exposure determined by nitrite actinometry to the clear-sky photon exposure
32 between 330-380 nm determined by the Simple Model of the Atmospheric Radiative Transfer of
33 Sunshine (SMARTS) model version 2.9.5¹ ([https://www.nrel.gov/grid/solar-](https://www.nrel.gov/grid/solar-resource/smarts.html)
34 [resource/smarts.html](https://www.nrel.gov/grid/solar-resource/smarts.html)) for the days each photochemical experiment was conducted. Data used for
35 these calculations are presented in Table S1.

36 The SMARTS hourly spectral irradiance (local time 07:00–17:00) for each irradiation
37 day was modeled following the protocol in Zhu and Kieber.² Two input parameters were used in
38 the SMARTS model: aerosol optical depth at 550 nm (AOD_{550nm}) and total column ozone
39 concentrations. The daily AOD_{550nm} was from the Moderate-Resolution Imaging
40 Spectroradiometer (MODIS) and the total column ozone concentrations were from the Aura
41 Ozone Monitoring Instrument (OMI) monthly averaged data. Both the ozone and AOD_{550nm} data
42 were from NASA’s Goddard Earth Sciences Data and Information Services Center
43 (<https://disc.gsfc.nasa.gov/>).

44

45

46

47

48

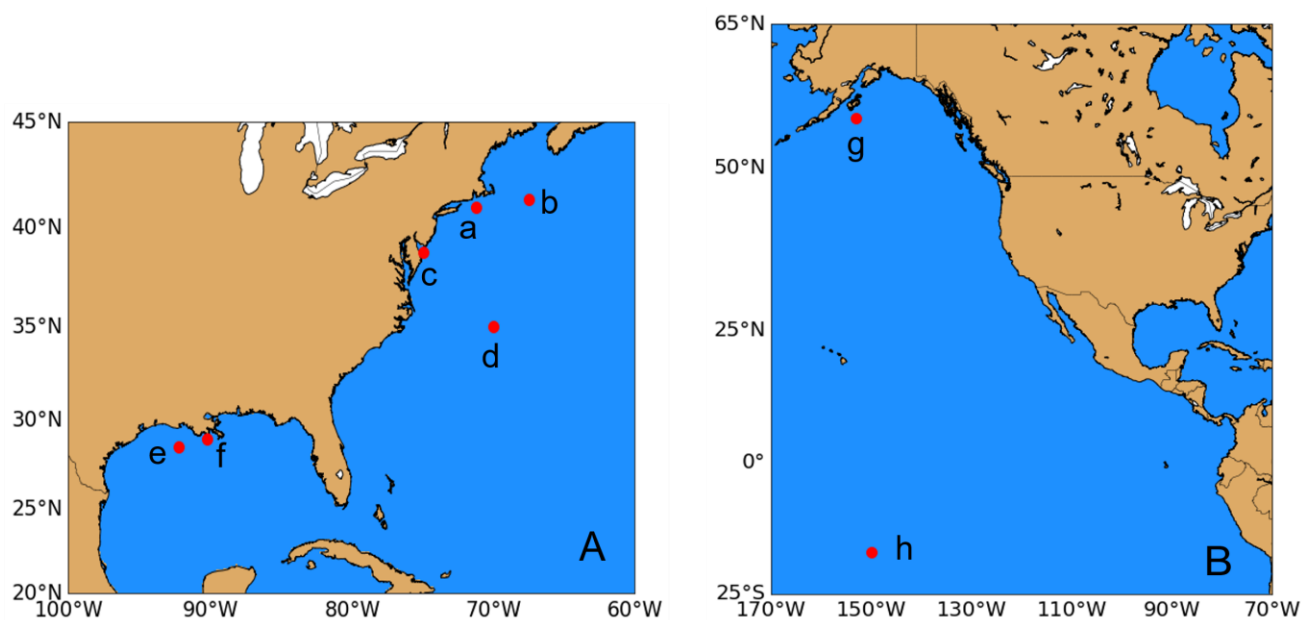
49 **Table S1** Data used to calculate average, clear-sky photochemical production rates. All irradiations were performed in Syracuse NY,
 50 except for the Mo'orea samples that were irradiated at the Gump Research Station in Mo'orea, French Polynesia. Nitrite actinometry
 51 and the SMARTS model integrated photon exposure between 330-380 nm. GOM denotes the Gulf of Mexico

Irradiation dates	Sample	Hours irradiated	Acrylate produced (nM)	Nitrite photon exposure ($\mu\text{mol quanta cm}^{-2}$)	SMARTS photon exposure ($\mu\text{mol quanta cm}^{-2}$)	Nitrite/SMARTS	Clear-sky rate (nM h^{-1})
April 7	Mo'orea Pacific Ocean	10.0	0.51	225.2	259.8	0.867	0.059
April 16-17	Mo'orea coral reef	20.0	0.66	405.5	491.7	0.825	0.040
April 18-20	Mo'orea Pacific Ocean	30.0	1.34	580.7	726.7	0.799	0.056
April 24-25	Mo'orea coral reef	20.0	0.94	309.4	468.7	0.660	0.071
August 20	GOM coastal	8.5	1.16	231.8	244.4	0.948	0.144
August 24	Delaware Estuary	9.0	0.95	236.5	242.6	0.975	0.108
September 4	Georges Bank	8.6	0.88	208.8	223.4	0.935	0.109
September 10	GOM open ocean	8.8	0.48	206.9	214.2	0.966	0.056
September 20	North Pacific Ocean	8.0	0.47	176.2	188.6	0.934	0.063
September 24	coastal Rhode Island	8.0	0.79	161.4	180.3	0.895	0.110
October 23-25	Sargasso Sea	18.5	0.47	236.8	317.5	0.746	0.034

52

53

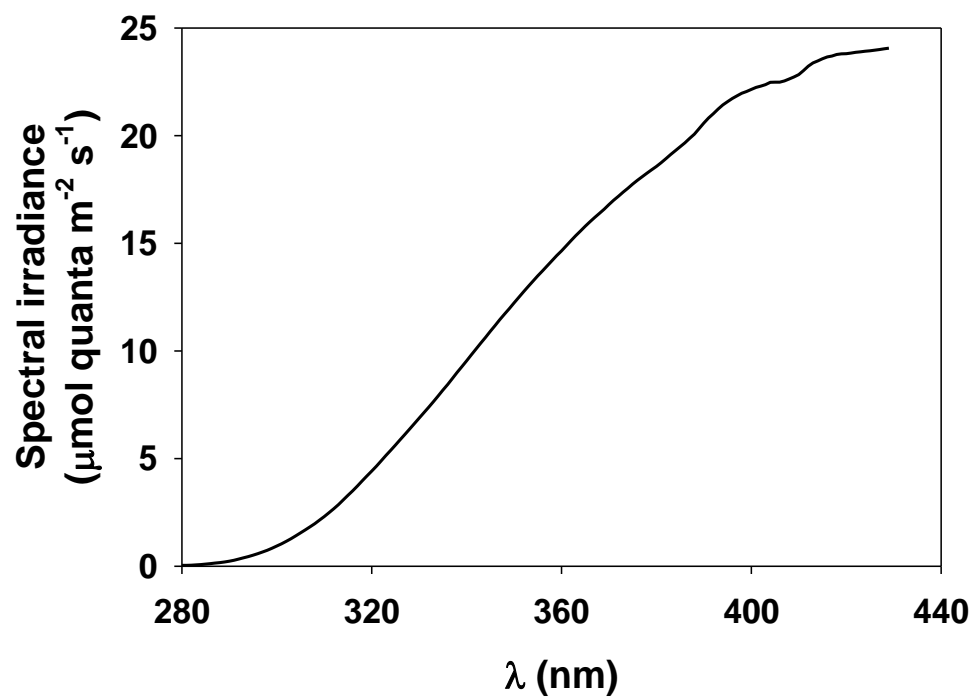
54



55

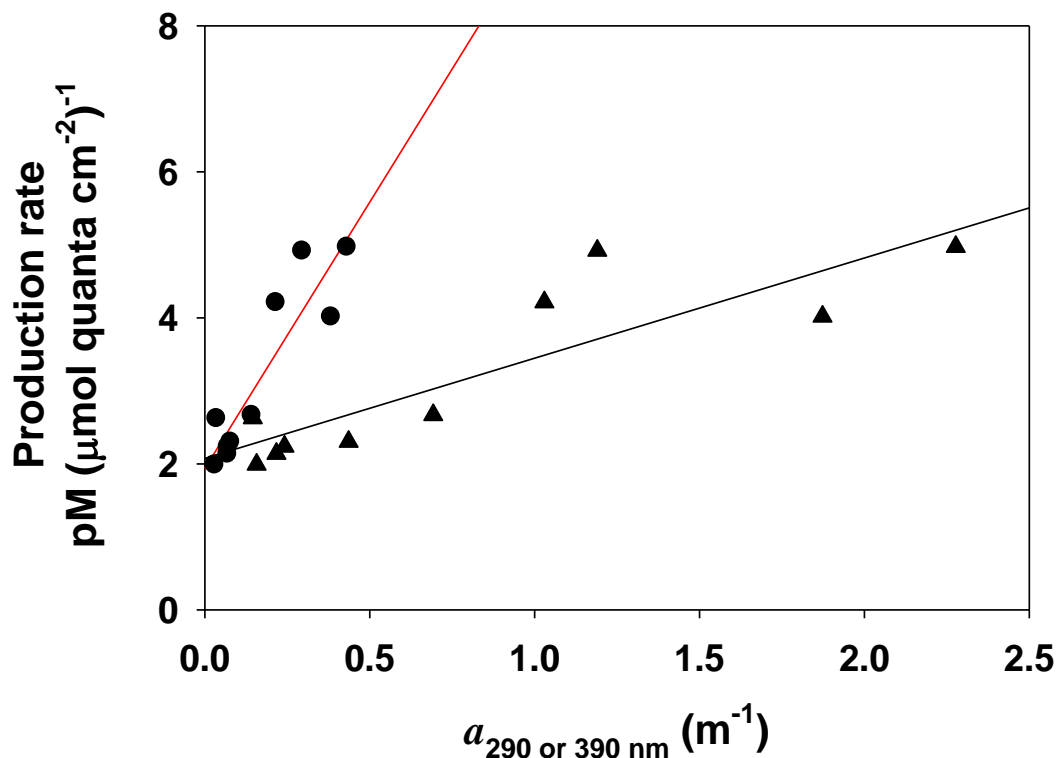
56 **Figure S1** Hydrographic stations in the (A) Atlantic and (B) Pacific Ocean where samples were
57 collected for photochemical experiments. Station notation: a, coastal Rhode Island; b, Georges
58 Bank; c, mouth of the Delaware Estuary; d, Sargasso Sea; e, Gulf of Mexico, open ocean; f, Gulf
59 of Mexico, coastal; g, North Pacific; h, coral reef and Pacific Ocean waters off the island of
60 Mo'orea, French Polynesia.

61



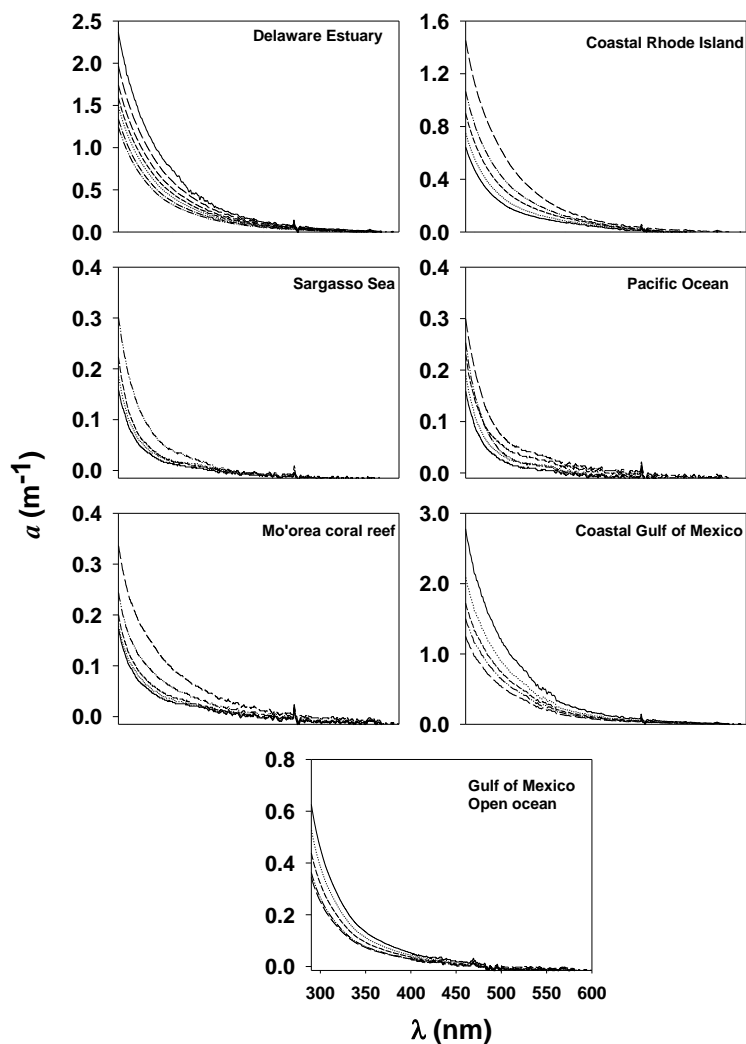
62 **Figure S2** Spectral irradiance output from the 300 W xenon lamp between 280 and 430 nm after
63 it passed through Milli-Q water to remove IR and a Pyrex plate to remove UV radiation less than
64 290 nm.

65



66

67 **Figure S3** Nitrite-based photochemical production rates of acrylate in the same samples shown
 68 in Figure 2 plotted against the CDOM absorption coefficient at 290 ($a_{290\text{nm}}$, triangle) or 390 nm
 69 ($a_{390\text{nm}}$, circle). The solid black and red lines are the best fit from linear regression analysis. The
 70 slopes and y-intercepts \pm std errors are: 1.37 ± 0.27 pM m ($\mu\text{mol quanta cm}^{-2}$)⁻¹ and 2.08 ± 0.30
 71 pM ($\mu\text{mol quanta cm}^{-2}$)⁻¹ for 290 nm (black line) and 7.29 ± 1.18 pM m ($\mu\text{mol quanta cm}^{-2}$)⁻¹ and
 72 1.94 ± 0.26 pM ($\mu\text{mol quanta cm}^{-2}$)⁻¹ for 390 nm (red line).

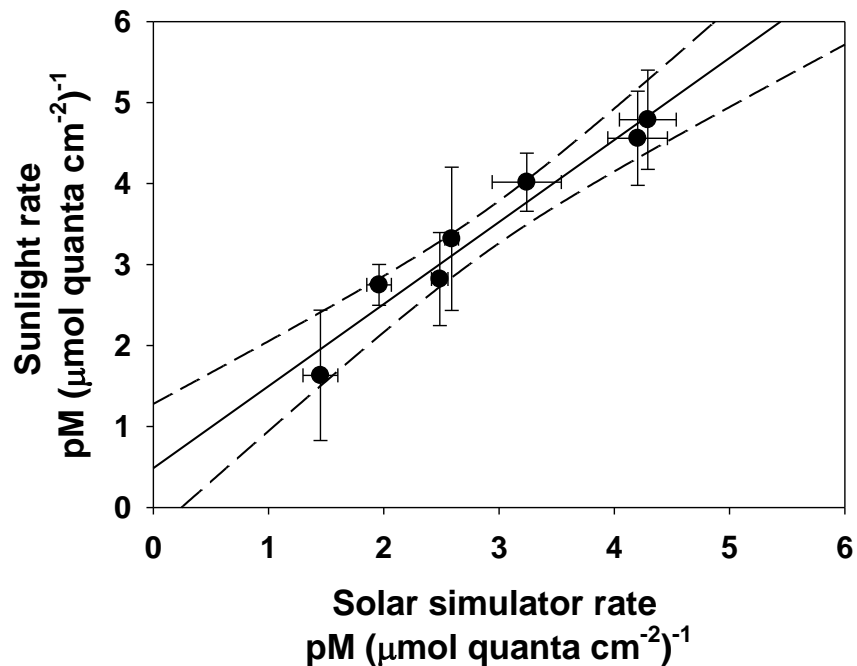


73
 74 **Figure S4** Decrease in the wavelength-dependent CDOM absorption coefficient during the
 75 irradiation of seawater samples using the solar simulator. For each seawater sample,
 76 wavelength-dependent absorption coefficients decreased from the initial spectrum to subsequent
 77 spectra at irradiation times of 2, 4, 7, and 10 h. All absorbance spectra were determined using an
 78 Ocean Optics spectrophotometer (model, SD-2000). The hourly photon exposure between 330
 79 and 380 nm as determined by nitrite actinometry in the quartz flasks was 0.22 ± 0.01 mmol
 80 quanta cm^{-2} .

81

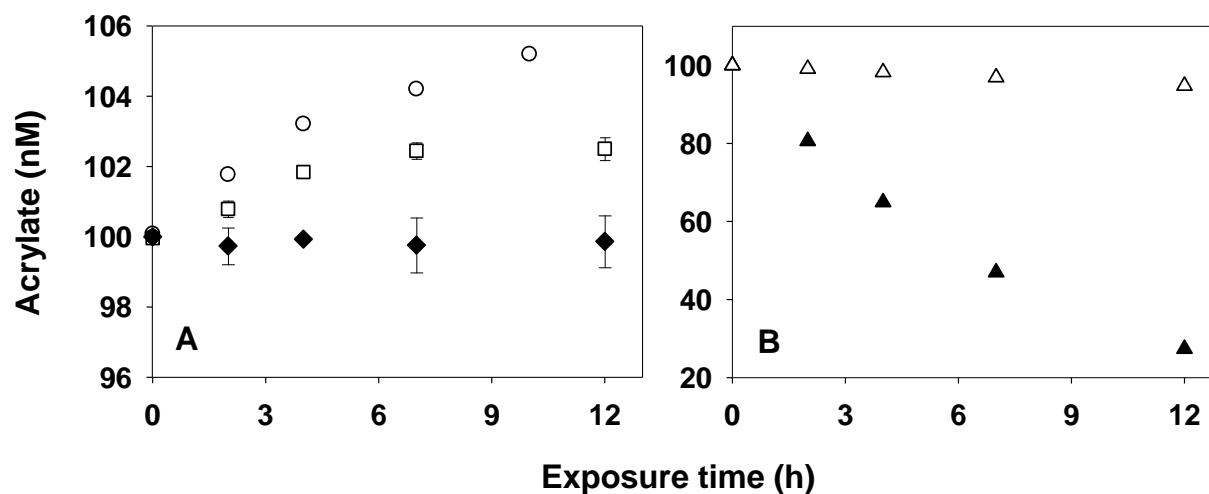
82

83



84

85 **Figure S5** Acrylate photoproduction rate determined in seawater samples exposed to sunlight
86 plotted against the rate determined in the same seawater samples exposed to the solar simulator.
87 Both rates were calculated based on the photon exposure determined by nitrite actinometry. The
88 solid line is the best fit line determined from linear regression analysis with a slope \pm std error =
89 0.94 ± 0.09 , a y-intercept \pm std error = -0.32 ± 0.33 pM ($\mu\text{mol quanta cm}^{-2}$)⁻¹, and $r = 0.98$. The
90 dashed lines denote the 95% confidence interval. Vertical and horizontal error bars denote the
91 standard deviation of replicate samples ($n = 3$ or 4).



92

93 **Figure S6** (A) Observed photochemical production of acrylate in 0.2 μm -filtered seawater

94 samples collected from coastal Rhode Island (circles) and the Sargasso Sea (squares) exposed to

95 the solar simulator for up to 12 h. Solid diamonds denote the observed change in the acrylate

96 concentration in Milli-Q water during exposure to the solar simulator for 12 h; the initial acrylate

97 concentration used in the Milli-Q water experiment was 100 nM. (B) Modeled photochemical

98 loss of 100 nM acrylate using the published first-order rate constant ($k_{\text{photolysis}}$) of $3 \times 10^{-6} \text{ s}^{-1}$ (Wu

99 et al.³; solid triangles) and $1.3 \times 10^{-7} \text{ s}^{-1}$ (Bajt et al.⁴; open triangles). The Bajt et al.⁴ $k_{\text{photolysis}}$ was

100 based on 15% loss of acrylate after exposure of a seawater sample to sunlight for 30 days

101 assuming first-order kinetics. The Wu et al.³ and Bajt et al.⁴ $k_{\text{photolysis}}$ rates constants were

102 normalized to the solar simulator spectral output between 330 and 380 nm (~ 7.5 suns). For all

103 solar simulator experiments, the hourly photon exposure between 330 and 380 nm was $0.22 \pm$

104 $0.01 \text{ mmol quanta cm}^{-2}$.

105

106

107

108 References

- 109 (1) Gueymard, C. A. Parameterized transmittance model for direct beam and circumsolar
110 spectral irradiance. *Sol. Energy* **2001**, *71*, 325–346.
- 111 (2) Zhu, Y.; Kieber, D. J. Global model for depth-dependent carbonyl photochemical
112 production rates in seawater. *Global Biogeochem. Cy.* **2020**, *34*, e2019GB006431.
- 113 (3) Wu, X.; Liu, C.-Y.; Li, P.-F. Photochemical transformation of acrylic acid in seawater.
114 *Mar. Chem.* **2015**, *170*, 29–36.
- 115 (4) Bajt, O.; Šket, B.; Faganeli, J. The aqueous photochemical transformation of acrylic acid.
116 *Mar. Chem.* **1997**, *58*, 255–259.
117
118